Synthesis of stable zinc oxide based catalysts for carrying out direct dehydrogenation of methanol to obtain (a) anhydrous formaldehyde and (b) highly selective hydrogen as by-product

Ankur Ghosh Chowdhury[1], Diana Deutsch[1], Ulrich Arnold[1], Jörg Sauer[1], Michael Bender[2]

[1] Institute of Catalysis Research and Technology (IKFT), Karlsruhe Institute of Technology (KIT), Hermann-von-Helmholtz-Platz 1, 76344 Eggenstein-Leopoldshafen

[2] BASF SE, Carl-Bosch-Straße 38, 67056 Ludwigshafen am Rhein, Germany

Abstract

There is a growing demand for renewable hydrogen in recent years with climate change attaining one of the highest priorities in today's industrialized societies. In industry, a significant amount of hydrogen is used in the methanol (CH_3OH) production. Successively, the produced methanol is used to manufacture formaldehyde (HCHO), which is one of the most extensively used raw materials for further synthesis of many other types of chemicals. However, most of these synthesis routes require its anhydrous form. Therefore, the currently and most widely used industrial oxidative dehydrogenation processes are disadvantageous, because of the formation of water during the manufacturing process. Not only is the separation chemistry of formaldehyde-water-methanol mixture a complex unit operation, but it is also relatively energy intensive [1]. Moreover, the hydrogen used in the beginning of the supply chain to produce methanol is lost, since it reacts to water.

The topic of direct dehydrogenation is therefore of real interest, because the two main products, viz. anhydrous monomeric formaldehyde and hydrogen are commercially of great interest. Zinc oxide (ZnO) is known to catalyze the direct methanol dehydrogenation [2–4]. However, the volatilization of ZnO at high temperatures is a major problem leading to a significant drop in the catalyst activity over time [3]. In this investigation, we initially compare the dehydrogenation chemistry of ZnO catalyst to the methanol pyrolysis, wherein the formed hydrogen and water was also quantified. To the best of our knowledge, a very few number of studies have been published till date catering to quantification of the trace amount of water formed during the dehydrogenation reaction [5]. All types of ZnO catalysts yielded a maximum of 0.8 vol% water inside the investigated temperature range. Experiments were carried out to stabilize activity of the catalyst with help of mild oxidizing agents, one of them being carbon dioxide (CO_2). Although a minimal stabilizing effect was observed, it did not completely hinder the catalyst deactivation. Consequently, focus was laid upon binding the ZnO chemically to silica support matrix by applying different manufacturing as well as heat-treatment (calcination) methods. A Time On Stream (TOS) study revealed a higher stability of the new catalyst, which surpasses stability of the ZnO catalyst with a constant methanol conversion and formaldehyde selectivity.

Introduction

A major task undertaken by the global political committees is to set the goal of a net-zero emission society by 2050 [6, 7]. For chemical industry, which is the third largest direct CO_2 emitter [8], this could mean recycling the emitted CO_2, where various basic chemicals (with C,H & O in their structure) can be manufactured in combination with H_2. For example, methanol (CH_3OH) is currently synthesized from CO_2, CO and H_2 at pressures from 50 to 100 bar and temperatures between 200 and 300 °C using $Cu/ZnO/Al_2O_3$ as catalyst. From which, approximately 30% caters to the single major usage, i.e., the production of formaldehyde [9]. The IEA predicts an increased CO_2 footprint in methanol production from 222 Mt/p.a. in 2020 to 269 Mt/p.a. by 2025 [8]. Therefore, manufacturing methanol completely with the help of recycled CO_2 would have a significant impact on the chemical sector alone in directly diminishing the GHG emissions. Although, recycling CO_2 is not just the only way of increasing sustainability and energy efficiency of industrial processes. During production of formaldehyde from methanol, one of the major side-products is water [1]. Currently industrially practiced processes include the silver contact process (with silver catalyst) and the formox process (iron

oxide-molybdenum oxide catalyst). In both processes, synthesis happens by means of two different routes, viz. through

    a. partial oxidation of methanol

$$CH_3OH + \frac{1}{2} O_2 \rightarrow HCHO + H_2O$$
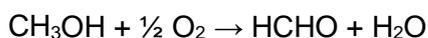
    b. direct dehydrogenation of methanol

$$CH_3OH \rightarrow HCHO + H_2$$

The partial oxidation route drastically reduces energy efficiency of the process because, the energy dense hydrogen used in manufacturing methanol in the beginning is thereby lost and converted to its more stable form, water. Consequently, the topic of direct dehydrogenation of primary alcohols and alkanes is of a significant relevance in process industry, due to the fact that the dehydrogenation chemistries are usually moderate to high endothermic reactions requiring relatively high temperatures [10]. It is important to mention here that, provisions have to be made to install a consecutive utility plant for anhydrous formaldehyde, since the molecule is very reactive and also unstable outside a specific range of temperature [11]. Hereby, one can imagine a manufacturing plant for generation of in-situ anhydrous formaldehyde from methanol and its subsequent utilization in the next step for manufacturing widely used formaldehyde derivatives like trioxane [12].

Pure zinc oxide is one of the very few materials known to be active towards the direct dehydrogenation chemistry of primary alcohols and alkanes [4, 13]. Recently, a paper has been published, where application of bulk gallium oxide (Ga_2O_3) material enabled a direct dehydrogenation of methanol, with an initial formaldehyde selectivity of 77% alongside a methanol conversion of 72% [14]. However, in case of bulk ZnO these values are much lower with initial selectivity of being 75% with only 10% methanol conversion [15]. Moreover, the high temperatures and a reducing atmosphere causes a relatively fast deactivation of both the above-mentioned catalysts in a very short time. In case of ZnO, the catalyst is reduced to metallic zinc, which then accumulates at the colder reactor outlet, thus leading to loss of active zinc species from the catalyst bed [15]. Previous efforts show that, manufacturing ZnO from different precursors, viz. zinc acetate, zinc nitrate or zinc chloride, led to different BET surface areas along with different activities [13]. Apart from application of different manufacturing techniques, efforts were undertaken to physically support bulk ZnO with typical support materials such as silica, alumina or titanium, to circumvent the volatility problem. Here, silica was the most effective support material with a significant improvement in catalyst activity as well its stability [16, 17].

In this study, we initially investigated the zinc oxide catalyst by physically supporting it with fumed silica. Although, in a harsh reductive environment the catalyst suffered serious deactivation, again due to catalyst volatility at high temperatures. Experiments were focused on in-situ re-oxidation of the reduced metallic zinc with help of CO_2 and O_2. Application of minimal O_2 in feed produced relatively high amounts of water as by-product, whereas application of CO_2 as a mild oxidizing agent was observed to slow down the zinc reduction (for one specific CO_2:CH_3OH concentration and reaction temperature), similar to investigations from Jung and his coworkers [3].

Since these measures did not lead to a complete overall stability of any manner, diverse efforts were undertaken to chemically bind the catalyst material to its support. Here, the interaction of zinc oxide with different support materials is a topic, which has been extensively investigated in past. Various applications of zinc silicate [18–20], zinc aluminate [21–25] as well as zinc titanate [26–28] as a spinel material can be found, primarily all across photo catalysis and in the electronics industry. Zinc titanate ($ZnTiO_3$) is a well-known sorbent candidate for high temperature hydrogen sulfide (H_2S) removal from exhaust gases of a coal gasifier [29]. Since

temperatures of the exhaust gases are as high as 650 °C, a stable form of zinc oxide has to be implemented. Therefore, by chemically binding TiO_2 to ZnO matrix, the reduction of zinc oxide could be hindered significantly. Analogous to this, volatility problem of the bulk ZnO can also be positively influenced by understanding its interactions with the SiO_2 material. Such an effect is also known as strong metal-support interaction and is a well-researched field of study in the branch of material science [30]. There are various phases of zinc silicate, which exist in resonance to the base material depending on formation and concentration of ZnO and SiO_2. Two of these are; zinc metasilicate/bisilicate ($ZnSiO_3$) and willemite or zinc orthosilicate/monosilicate (Zn_2SiO_4). Some of these are even found naturally in the ore and mines of zinc [31]. Presence of impurities inside their structures enable physical and chemical properties of the material to vary largely, in some cases leading to a wider band of emission spectrums, an enhanced thermal and electrical conductivity or in some cases very good dielectric properties have also been observed [32]. The structure of zinc silicate material allows its widespread usage as a host matrix for various dopants. Although, manufacturing these materials in laboratory could be a very challenging task. Sagou and coworkers have made constant efforts in 1980s to manufacture the zinc silicate in Zn_2SiO_4 structural form [13, 16]. In one study they reported an amount of 43.1 wt% of Zn and 21.2 wt% Si in the catalyst matrix by performing ICP elemental analysis [33]. This suggests that the material manufactured had a chemical formula of $Zn_1Si_{1.14}O_{3.38}$, rather than the targeted Zn_2SiO_4 catalyst.

Out of the various available synthesis methods, during this study we have applied the sol-gel method to synthesize all the zinc silicate materials [34]. Thereby, usage of different calcination methods and temperatures enabled varied structure specific characteristics of the same material. Simultaneous to the catalyst activity tests, characterization of the material was executed. XRD and EDX techniques were used to investigate phase structures and surface elemental composition respectively, thereby disclosing some physical characteristics of the material. Physisorption experiments were also undertaken for measuring BET surface area. For investigation of chemical properties, bulk composition was characterized with the help of ICP-OES method before and after the reaction, to quantify the loss of zinc from catalyst matrix. During some experiments, deposition of carbonaceous species was also observed. Here TGA method with synthetic air (20.5% O_2) was implemented to burn off the coke and determine the amount during a specific TOS. The synthesis and characterization methods have been described in detail in the following sections of this investigation.

Experimental section

Catalyst preparation

ZnO nanopowder (Sigma-Aldrich, <100 nm particle size) was directly obtained for catalytic tests, where the powder was calcined at 600 °C in static air for 5 hours. Before application on the fixed bed, 5 wt% of the powder was mixed with fumed silica (SiO_2, Sigma-Aldrich), pressed and sieved. The sieve fraction in between 400 – 600 µm was used throughout all experiments, even for the zinc silicate trials. A single ZnO catalyst was tested during this study, whose sample name was ZnFS/SA1.

For preparation of zinc silicate materials, the following chemicals were exactly used as they were commercially procured without undergoing any pre-treatment; zinc nitrate hexahydrate ($Zn(NO_3)_2 \cdot 6H_2O$, Sigma-Aldrich, reagent grade 98%) and tetraethyl orthosilicate (TEOS, Sigma-Aldrich, for synthesis) were used as precursors for obtaining zinc silicate based catalyst. The molar ratio of Zn to Si was fixed at 2. The zinc precursor was dissolved in a round bottom flask using ethanol as solvent. To this, the required amount of TEOS was fed in, while constantly stirring the solution inside the flask. All steps were performed in room temperature. After this, the pH of the solution was adjusted to 4, with help of nitric acid to activate the sol [35]. The solution was then allowed to stand at room temperature. Evaporation of the solvent took place at ambient temperature and with the help of natural air convection [32]. After a couple of days, the formed gel turned into a white powder, which is also known as gel desolvation effect [10]. This was thoroughly washed and then dried for 12 hours at 120 °C. To

undertake calcination, two types of ovens were utilized, viz. ovens with static & dynamic airflow. The prepared zinc silicate was calcined at 450 °C, 750 °C and 950 °C in both oven types to observe various material characteristics. Here the rate of heating was 5 °C/min with 5 hours of dwell time for the observed calcination temperatures. The various zinc silicates were named with the prefix, ZnSi. This was followed by the abbreviations SA or DA, which depicted the type of calcination procedure, viz. Static Airflow or Dynamic Airflow respectively. Lastly, numbers 2 to 5 represent the different end temperatures during each calcination procedure.

Catalyst characterization

Phase composition of differently calcined zinc silicate catalysts was determined by means of XRD with Cu-Kα (40mA, 45 kV) as the source of X-ray. Peak positions and profiles were then determined and fitted with the help of X'Pert Highscore software.

N_2 physisorption measurements were performed using a Quantachrome Novawin analyser. Prior to the measurements, samples were degassed to 130 °C with 20 h holding time. During the measurement, adsorption and desorption isotherms were recorded and the BJH fitting was applied to determine surface areas of all the tested catalysts.

In order to quantify elements on the surface of the material, SEM and EDX measurements were carried out with the help of a Zeiss V16 microscope. Thereafter, PhiZAF method was used to quantify the recorded maps. The software also automatically calculated atom percentages (at%) of respective elements from the measured weight percentages (wt%).

For characterization of chemical composition of the catalyst bulk, ICP-OES measurements were undertaken. An Anton Paar Multiwave 3000 instrument was used for sample preparation, where a maximum amount of 500 mg of sample was completely digested in concentrated hydrogen fluoride solution (40%). An Agilent 725 ICP-OES Spectrometer was then used to detect the ions, which were generated by ionizing the solution with help of an argon plasma. Here the flow rate of Ar was maintained at 15 l/min.

Lastly, TGA analyses of carbon deposited on the materials were performed to estimate the amount of carbon formed per unit time. Here, synthetic air (20.5% O_2) was used to heat 30 mg of sample at a rate of 10 °C min^{-1}. Here the end temperature was maintained throughout at 1000 °C.

Catalyst activity

The testing of catalysts was executed inside a fixed bed of quartz glass tube with 9 mm inside and 12 mm outside diameter. Temperature at the bed was measured directly with a thermoelement protected by a thin tube of quartz glass. A typical experiment always comprised 250 mg of catalyst material. The weighed catalyst was sandwiched in between two plugs of quartz wool and placed in isothermal zone of an electric oven. The oven was purchased from Horst GmbH, which served as the heating device for the reactor. The device had a total length of 550 mm, with a single heating zone, which was 450 mm long.

A specific amount of liquid methanol was fed by overpressure (under He 6.0), where the flow was measured with a Cori-flow mass flow meter (MFM). At downstream the MFM was attached to an evaporator, which was supported with a N_2 mass flow controller (MFC) used also as the process carrier gas (purity: 5.5). All instruments were purchased from Wagner Mess- und Regeltechnik. A second MFC was assigned to feed either CO_2 or synthetic air (purity of both gases: 5.5) into the feed. Actual amount of the flowing gas was dependent on upstream pressure of the MFC and the conversion factors were calculated with help of the online available Fluidat Software from Bronkhorst.

A gas chromatograph (GC) model 7890 from Agilent equipped with two thermal conductivity detectors (TCD) was used to determine and quantify the effluent gases. The dosing took place

by generation of under pressure on the analytic bypass line, which then forced the gases to flow through sample loops inside the GC. After sufficient purging with effluent gas from the process outlet, samples were released into two channels of the GC. The back TCD detector was supplied with Ar (purity: 6.0) as carrier gas to detect the permanent gas species (H_2, CO, CH_4 and CO_2), whereas He (purity: 6.0) was used in the front detector.

Calibration of water was carefully carried out with the help of a humidity measurement device and a psychometric chart. After complete calibration of main components of air, the value of relative humidity was used to determine humidity ratio. This furthermore revealed the concentration of water in a specific volume of air. This process was repeated three times at three different times of a day. The resulting correlation factor of these calibration points was 0.99959, which showed good accuracy of calibration.

A typical experiment was approached as follows, where an inert gas feed (N_2), was used in the beginning not only to purge the system, but also simultaneously to heat up reactor and the catalyst bed. After steady state, a specific stream of methanol was fed in. During all the tests, amount of methanol was kept constant at 5 vol%. For parameter optimization, temperature programmed experiments were carried out by varying the temperatures from 400 to 750 °C.

Results and discussion

Catalyst characterization

From table 1 it can be interpreted, that the different methods and temperatures of calcination had different effects on the catalyst characteristics. The zinc silicate powder, ZnSi/SA2 calcined at the lowest temperature showed the highest BET surface area just after the ZnO catalyst, ZnFS/SA1. This was expected, because thermal treatment at higher temperatures lead to sintering of the material and smaller pores merge and create larger pores inside the matrix [32]. It is also worth mentioning, that apart from the usage of an acid in sol-gel method instead of a base, the dynamic airflow method proved to be a better method for preparing catalysts with a higher pore volume.

Table 1: Sample nomenclature with measured physical properties of the various zinc oxide catalysts.

Samples	Calcination temperature, dwell time / °C, h	S(BET) / $m^2 \cdot g^{-1}$	Zn in bulk / wt% (fresh)	Zn on surface / wt% (fresh)	Zn:Si / ratio of at% (fresh)	Zn in bulk / wt% (spent)
ZnFS/SA1	550, 5	154.4	4.3	2	0.1	0.08
ZnSi/SA2	450, 5	58.4	57.5	65.7	3.3	40.6
ZnSi/SA3	750, 5	18.3	58.4	80.3	2	53.3
ZnSi/SA4	950, 5	8.5	56.6	71.3	1.3	53.5
ZnSi/DA5	900, 5	12.8	57.1	83.6	2.5	54.5

The usage of an acid increases the hydrolysis rate of sol, which not only leads to a lesser branched gel formation, but it is also related to more pore volume [10]. The later phenomenon can be explained through an uneven heat and mass transport in case of the static air type of oven, where achieving a steady state requires more time and it is prone to small disruptions caused due to changes in air pressure of its surroundings [36]. The surface weight percentages of zinc was higher than those in material bulk. In the bulk, zinc silicate material largely corresponds to the targeted Zn_2SiO_4. The theoretical weight percentages of Zn, Si and O are 58.68%, 12.6% and 28.72%, respectively. Table 1 shows, that the samples prepared through sol-gel procedure exhibit a maximum deviation of 3.5% from the targeted material after performing calcination. On, the other hand, the wt% of Zn on the surface measured with the help of EDX method, showed a maximum deviation 42% for the ZnSi/DA5 catalyst. The EDX measurements also showed that ZnFS/SA1 and ZnSi/DA5 had a rather inhomogeneous

distribution of the active component (Zn) in their structures, which can be seen from the figure 1. The figure shows presence of Zn, Si, O and C elements on the material surface represented by the various colors. In case of both the catalysts, the distribution of Zn was rather uneven, comprising of small dense patches. Here, it is important to note, that only one measurement for each of these catalyst was carried out. Hence, it also explains the huge deviation of almost 40% in the surface Zn wt% for the ZnSi/DA5 catalyst material. However, contrary to the material manufactured by Sagou [13], this was already a huge improvement in regards to synthesis of the targeted catalyst material. Results of the bulk material chemical composition was also supported by observing the different phases of zinc silicate material, where a higher calcination temperature of the material not only increased the material crystallinity, but also the more phases of the desired Zn_2SiO_4 could be observed at 950 °C and above [34]. Please refer to the figure 2 for information on these XRD analyses.
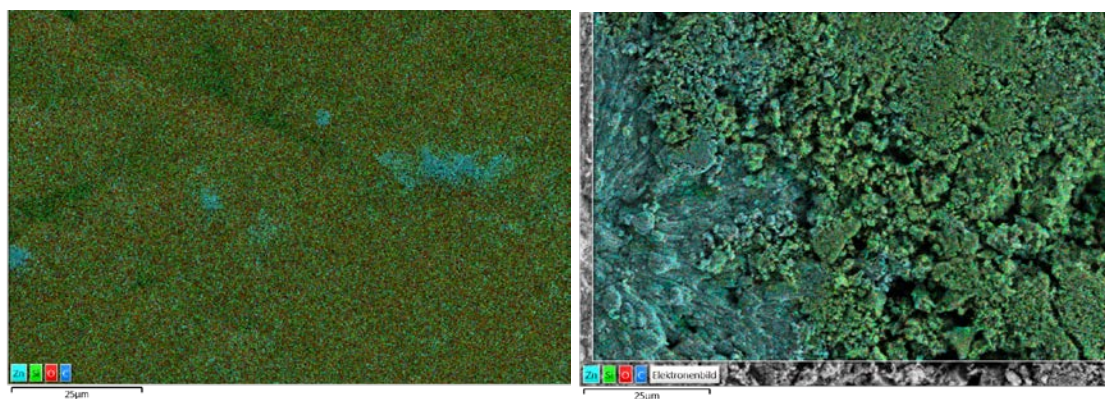
Figure 1: EDS (energy-dispersive X-ray spectroscopy) measurements superimposed on the SEM images to look at the elemental composition on the surface of ZnFS/SA1 (on the left) and ZnSi/DA5 (on the right).
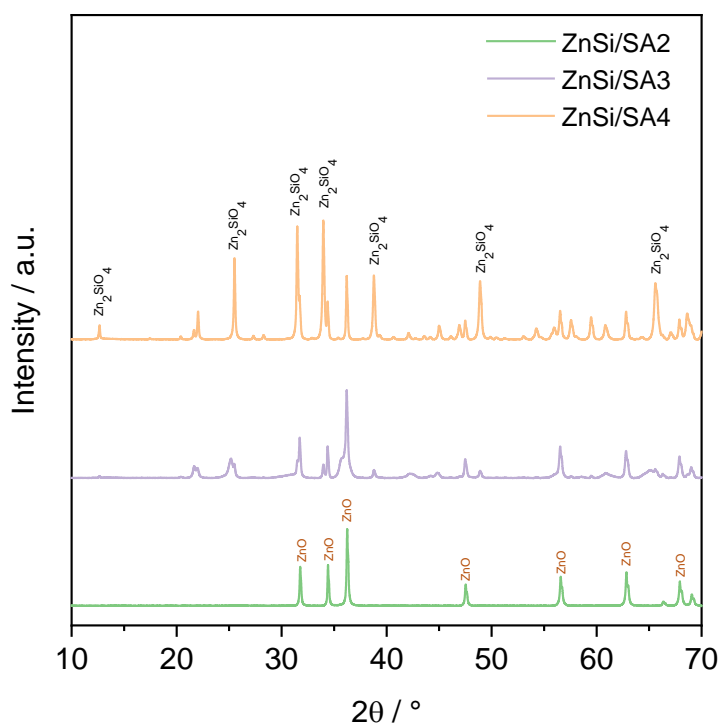
Figure 2: XRD patterns of zinc silicate samples calcined in static air oven at temperatures of 450, 750 and 950 °C.

Catalyst activity

ZnFS/SA1 was the first catalyst to be tested for looking at the products of methanol dehydrogenation chemistry. Figure 3 shows a typical product spectrum obtained with the pure ZnO material. An expected increase in the methanol conversion was represented through this test, until the temperatures were high enough for a fast ZnO reduction leading to a fall in the methanol conversion. By the end of experiments, accumulation of metallic zinc could be observed, proving the volatility of zinc oxide in a reducing atmosphere. Apart from that, figure 4 shows the main products of direct dehydrogenation. Here, it can be seen that the catalytic yield of anhydrous formaldehyde throughout the investigated temperature ranges (400 – 700 °C) always exceeded the HCHO yield from the methanol pyrolysis process, which is normally performed at 700 – 950 °C. During methanol pyrolysis, significant conversions of methanol only appear at temperatures exceeding 700 °C [37]. The selectivity of hydrogen in comparison to water for both the systems was almost 99%, with a maximum yield of 0.8% water for the ZnFS/SA1 catalyst. Through bulk elemental analysis, it was observed that, the spent ZnFS/SA1 catalyst had lost 98.13 wt% of zinc from its matrix after 8 hours of TOS. As a corrective measure, a certain amount of O_2 was introduced in the feed along with methanol and N_2 carrier gas. The ratio of O_2:CH_3OH was varied in the between 3.3, 2 and 1. All three feeds yielded water as product for a WHSV of 364.6 h^{-1} in the temperature range of 400 – 750 °C. Naturally, the highest amount of water was produced in an oxygen rich feed mixture (O_2:CH_3OH = 3.3) and at 750 °C, where the oxidation of H_2 took place majorly in the gas phase [38].
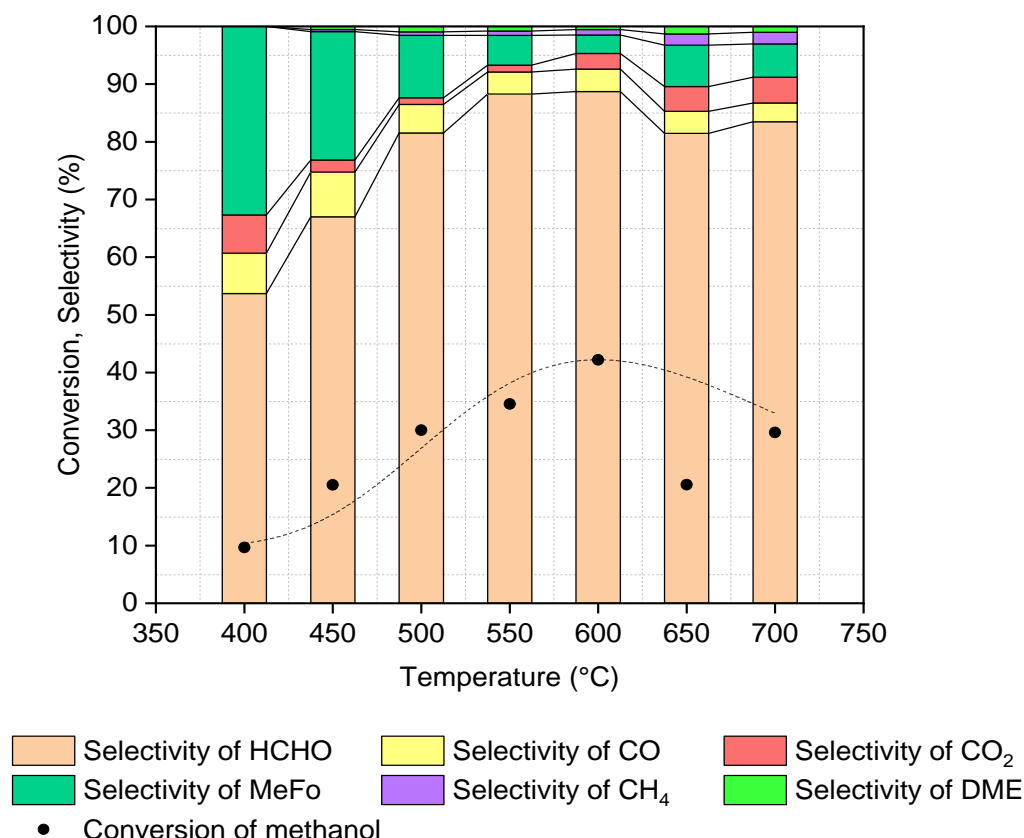
Figure 3: Conversion and selectivity of methanol and its various reaction products respectively versus reaction temperature for the ZnFS/SA1 catalyst system.
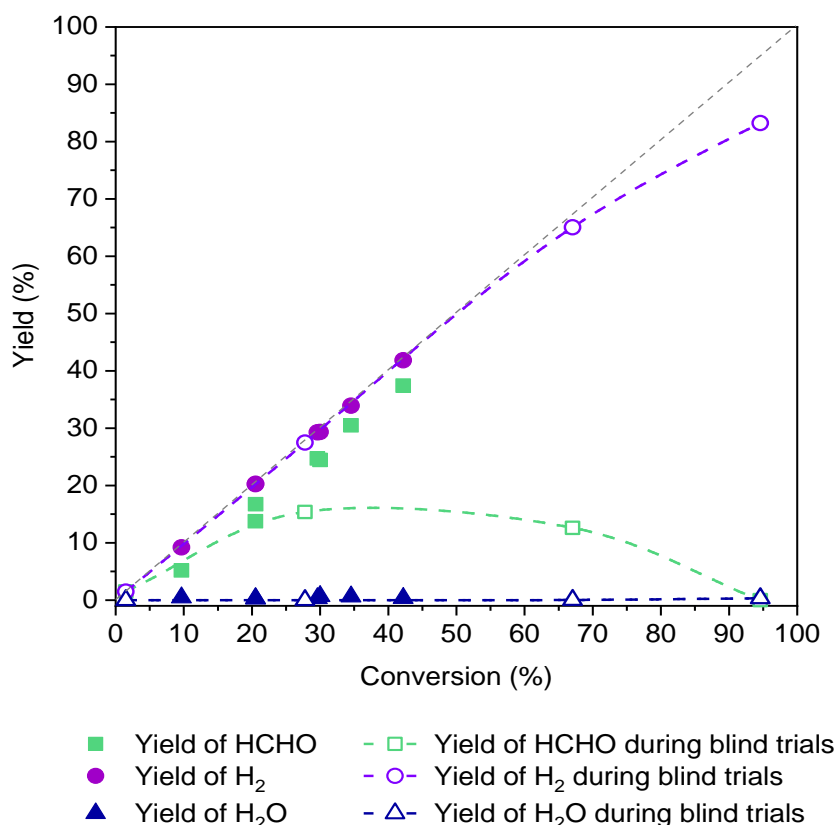
Figure 4: A comparison of conversion of methanol versus yield of formaldehyde, hydrogen and water in between methanol pyrolysis and ZnFS/SA1 catalyst system.

Since, trials with oxygen led to water formation, CO_2 was introduced into the feed, as a mild oxidizing agent. Addition of CO_2 was carried out mainly for two temperatures of interest, viz. 500 and 550 °C, indicated in the figure 5 with blue and red lines. Below this temperature, methyl formate (MeFo) dominated the product spectrum, whereas above 550 °C, deactivation of the ZnO was rather accelerated (also in presence of CO_2). CO_2:CH_3OH ratio in the feed was varied once to 0.8 and then to 1.4. Again, full deactivation of the catalyst could not be completely hindered. Moreover, the reduction could only be slowed down at a temperature of 500 °C and a feed ratio of 0.8. The trend of these observations was in resonance with other investigations, where influence of CO_2 showed to diminish the reduction effect of ZnO [3, 39]. There were two major conclusions resulting from these investigations. The first that, CO_2 clearly blocks the catalytically active adsorption sites by occupying them, suggesting a probable interaction with ZnO. This can be proved through a lower initial methanol conversion in the presence of CO_2 (irrespective of its ratio to methanol) in comparison to when it was absent. Additionally, the second observation suggests that, CO_2 had a stabilizing effect on the ZnO catalyst. This effect is well known, but the exact reason is not quite understood, especially in the field of methanol dehydrogenation.

In propane dehydrogenation chemistry, CO_2 addition also shows a stabilizing effect, which can be attributed to less coke formation and therefore the catalyst remains relatively longer active [40]. Here, a Boudouard reaction is assumed to be taking place which would then explain the stabilizing effect of CO_2 [41].

   a. Boudouard reaction

$$CO_2 + C \leftrightharpoons 2CO$$
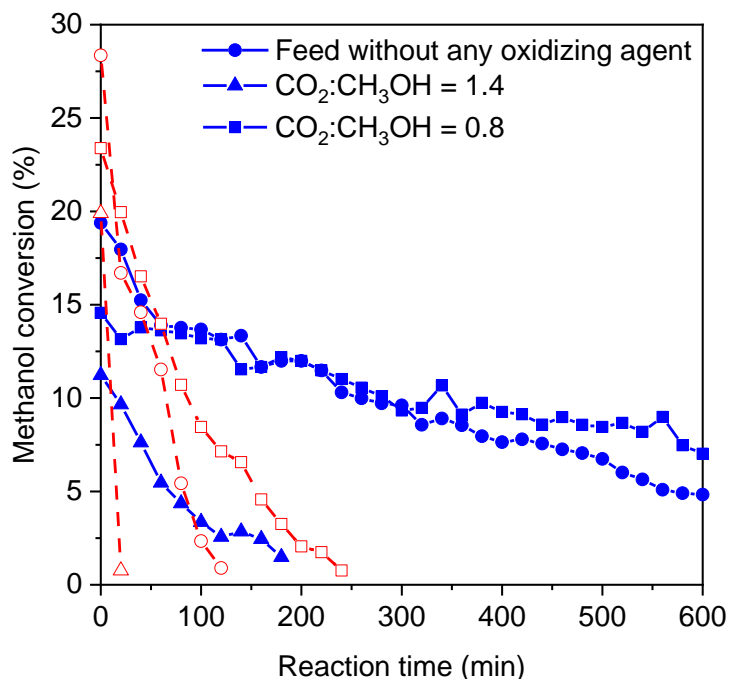
Figure 5: Reaction time versus methanol conversion at two different CO_2:CH_3OH ratio and temperature (500 °C (blue lines) and 550 °C (red dotted lines)).

The deactivation at 550 °C was fast, showing rather an adverse effect of CO_2 addition. Notably, here the worst performance was observed in presence of a CO_2 rich mixture where, not only the stability of catalyst was negatively affected, but also conversion of methanol was the lowest. Presumably, here the CO_2 not only blocked active ZnO sites to make a different chemistry, but a higher temperature caused a much faster ZnO to Zn reduction. Although a fitting explanation would only be possible through scrutinizing the amounts of different effluent gases. Moreover, presence of two C-species as raw material, made the analytical assessment more challenging. The pronounced concentration of CO and the diminished amount of CO_2 in effluent gases could therefore be roughly co-related to not only a bourdard reaction, but rather to a resulting oxidation reaction of Zn to ZnO [42].

The ZnSi/SA2 system deactivated almost as fast as the ZnFS/SA1. From the XRD measurement in figure 2 the reason becomes quite evident, where deactivation happens because of the ZnO in lattice structure, which lies freely without being bound to the silica. Moreover, the ZnSi/SA2 system had lost 30% Zn after 8 h TOS, whereas the ZnSi/SA3 had only lost 8.7%. The least reducible catalyst were the ones calcined at and above 900 °C. In figure 6, the activity of ZnSi/DA5 catalyst is depicted. Experiments with other zinc silicate catalysts showed the same product composition, however ZnSi/DA5 appeared to be the most stable and active of all. Thereby, comparing the product spectrum of the physically and chemically bounded supports (ZnFS/SA1 and ZnSi/DA5), one can clearly see that silica interacts with ZnO in a manner that the chemistry was not completely changed. The formation of small amounts of dimethyl ether (DME) was probably due to presence of a small density of acidic sites present in silica [43]. It is well known, that a direct dehydrogenation of methanol on ZnO catalyst is associated with formation of formate species [44]. The presence of basic sites lead to higher electro positivity, thereby favouring methyl formate and CO formation [15]. The trend here was same for both catalysts, where methyl formate formation was less pronounced at higher temperatures. The hypothesis from Sagou et al. is as follows; at higher temperatures, the formaldehyde route is favoured and this is also easily desorbed from surface [13]. Although, the presence of a nearby adsorbed hydrogen leads to formation of CO_2 and H_2, thereby extracting oxygen from the catalyst matrix. This was assumed to be the culprit reaction behind a fast ZnO deactivation mechanism [45]. Further characterization and in-situ or ex-situ

investigations are required to thoroughly understand the individual adsorption/desorption steps taking place on and inside the catalyst surface and bulk, respectively. The methanol conversion of ZnSi/DA5 was slightly lower compared to ZnFS/SA1 catalyst for the similar temperature region. The absence of free ZnO species can be the reason, which could explain this effect.
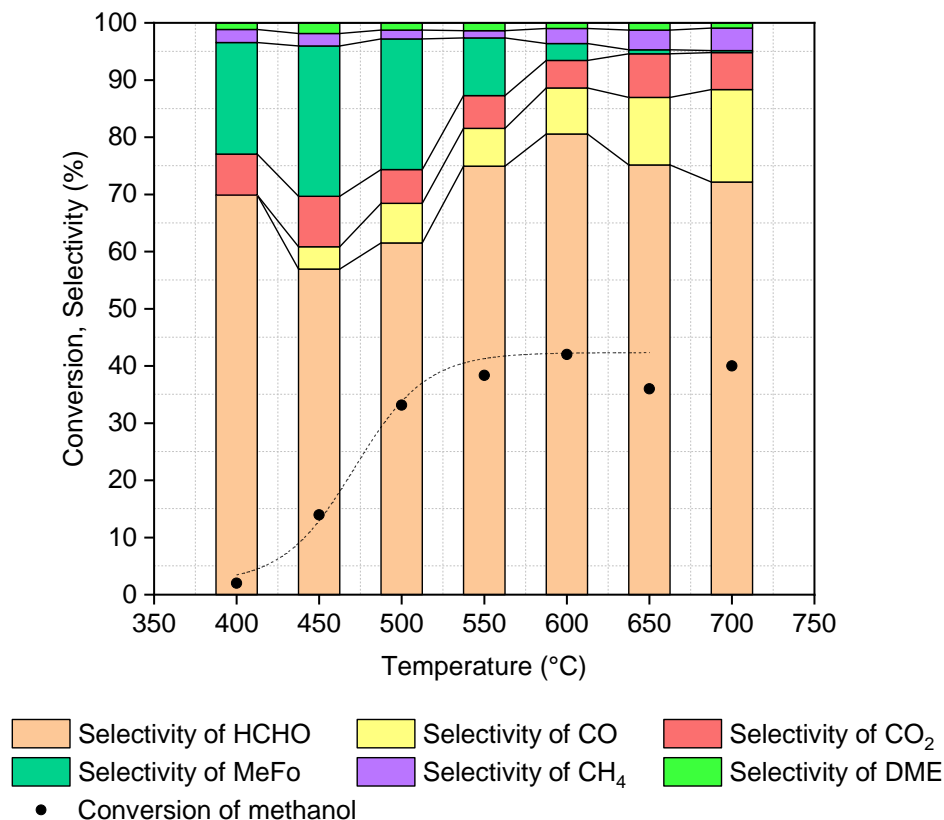
Figure 6: Temperature versus conversion and selectivity of various reaction products for the ZnSi/DA5 catalyst.

Initially, the reason for deactivation of the catalyst was unknown, since no single deactivation mechanism could be ascertained. Because of change in colour of the catalyst powder from white to black, we could confirm deposition of carbonaceous species. Therefore, TGA experiments were executed, where the deposited carbon was burnt away in presence of oxygen. After 8 h of TOS, there was 5.2% carbon deposits on the ZnSi/DA5 surface. Although, this measurement was performed, keeping a dehydrogenation chemistry in mind (where coking is a common phenomenon), it was assumed not to be the only reason for decrease in the catalyst activity. As discussed before, ICP-OES measurements enabled some insight about the loss of Zn, which occurred in every catalyst system. For the ZnSi/DA5 catalyst discussed here in detail, this value was only 4.5% after 8 h of TOS. Irrespective of this fact, the activity as well as catalyst lifetime was still not anywhere close to a practicable usage in industry. From figure 7, some very interesting observations could be made about these three catalyst systems, viz. ZnFS/SA1, ZnSi/SA4 & ZnSi/DA5.

It shows reaction time in hours on the x-axis versus conversion of methanol along with formaldehyde selectivity on the y-axis. The reaction temperature was fixed at 550 °C for this experiment. Out of all the effluent gases, only formaldehyde selectivity has been depicted in the diagram. The ZnFS/SA1 catalyst completely loses its activity in just two hours from the start of experiment. The ZnSi/SA4 and ZnSi/DA5 catalyst on the other hand show relatively more stability reaching almost stable conversions of 10% and 20% respectively. A common

phenomenon observed for both of these systems was the initial drop in methanol conversion. This was possibly because of the presence of free ZnO, which was then quickly reduced (similar to that of ZnFS/SA1) to zinc metal found in the end of reaction. After this stage, the ZnSi/SA4 catalyst showed a slow and steady fall in conversion. The selectivity of formaldehyde was same throughout with an average around 68%. After a steep fall in methanol conversion in the beginning, there was a rather slow and steady fall in the activity until 10 h of TOS for the ZnSi/DA5 catalyst.
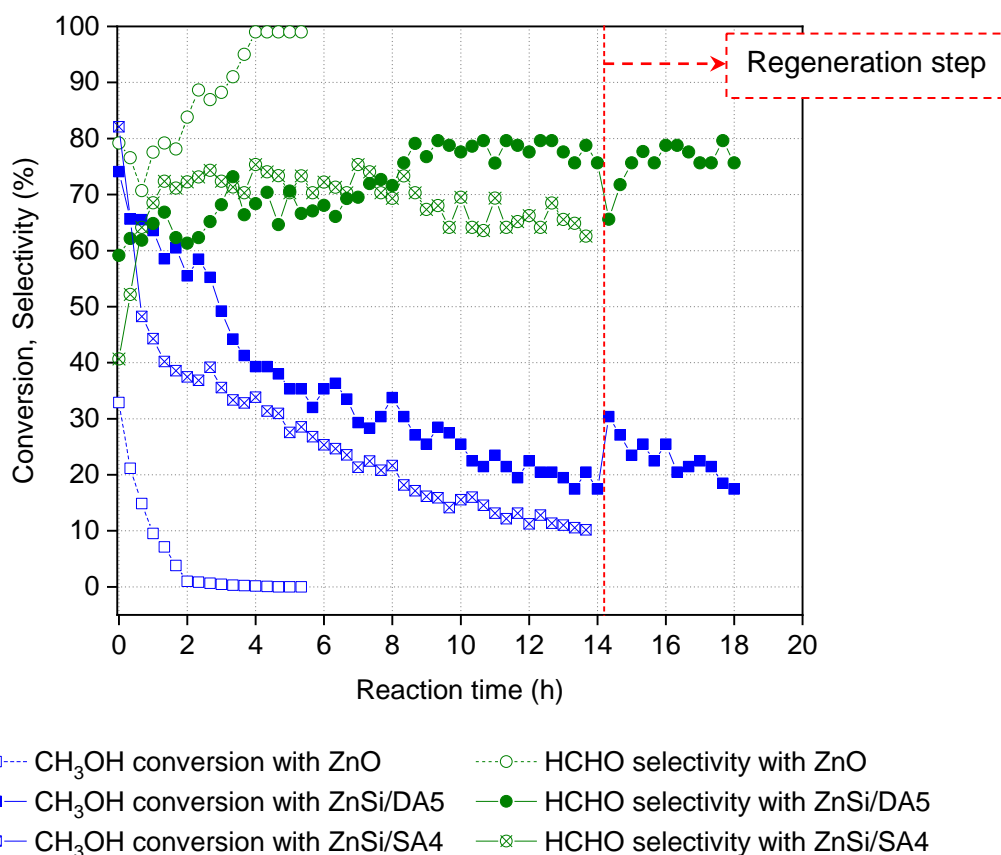
Figure 7: TOS experiments with zinc oxide and zinc silicate catalysts.

The catalyst was observed to be stable after this point. An attempt was made to burn away the coke, which had accumulated on the catalyst surface and at the bulk with time. Regeneration step composed of treating the system with synthetic air for couple of minutes. After this, the methanol stream was turned on again. The attempt was not successful to fully restore the previous activity of catalyst, where within two hours the methanol conversion dropped back to 20%. This furthermore concluded, that the deactivation of the catalyst was not just because of coking, but rather a mixture of Zn loss and coking both. Comparing the ZnSi/SA4 and ZnSi/DA5 catalysts, we also conclude that the material calcined by dynamic flow of air had more pore volume and this was also the probable reason for its slightly higher activity to decompose methanol.

Conclusion and comments on the potential scope of zinc silicate catalyst

From the study of the aforementioned catalyst systems, rough comments can be delivered regarding the potential scope of zinc oxide catalyst system. The zinc oxide catalyst is one of the very few materials, which bring about the direct dehydrogenation of methanol with formation of trace amount of water. The high volatility of the material leads to its fast deactivation, where a mild oxidizing agent like CO_2 was helpful in slowing down this process either by prevention of coke formation or by re-oxidation of zinc, which could not be completely

understood within the scope of this investigation. More experiments are required to comprehend this effect. Nevertheless, application of an acidic environment to the sol-gel method and then calcining the material in dynamic airflow at 900 °C or higher yielded a zinc silicate material, which showed a relatively high stability (with loss of only 4.5 wt% Zn in 8 h TOS). A steady methanol conversion of 20% was achieved accompanied with 80% formaldehyde selectivity in a completely reductive atmosphere. Therefore, this study lays down the first impressions of a material manufactured at one specific $ZnO:SiO_2$ ratio, to achieve approximately a higher Zn_2SiO_4, zinc silicate phase, which is known to be the more stable material for the methanol dehydrogenation chemistry.

References

References
1. Adam, W. Franz Helmut, Kronemayer, P. Daniel, D.P. Roman, R. Gänther, D. Walter, O.G. Armin, H. Albrecht (eds), *Ullmann's Encyclopedia of Industrial Chemistry* (Wiley-VCH Verlag GmbH & Co. KGaA, Weinheim, Germany, 2000)
2. S. Danwittayakul, J. Dutta, International Journal of Hydrogen Energy **37**, 5518 (2012)
3. K.-D. Jung, O.-S. Joo, S.-H. Han, S.-J. Uhm, I.-J. Chung, Catal Lett **35**, 303 (1995)
4. D. Kaiser, L. Beckmann, J. Walter, M. Bertau, Catalysts **11**, 869 (2021)
5. C.J. Baranowski, J. Brandon, A.M. Bahmanpour, O. Kröcher, ChemCatChem **13**, 3864 (2021)
6. D. Welsby, J. Price, S. Pye, P. Ekins, Nature **597**, 230 (2021)
7. S. Fankhauser, S.M. Smith, M. Allen, K. Axelsson, T. Hale, C. Hepburn, J.M. Kendall, R. Khosla, J. Lezaun, E. Mitchell-Larson, M. Obersteiner, L. Rajamani, R. Rickaby, N. Seddon, T. Wetzer, Nat. Clim. Chang. **12**, 15 (2022)
8. Tiffany Vass, Peter Levi, Alexandre Gouy, Hana Mandová, *Direct CO2 emissions from primary chemical production in the Net Zero Scenario, 2015-2030*, https://www.iea.org/reports/chemicals (2021)
9. U. Mondal, G.D. Yadav, Green Chem. **23**, 8361 (2021)
10. G. Ertl, *Handbook of heterogeneous catalysis* (Wiley-VCH; [Chichester : John Wiley, Weinheim, 2008)
11. S. Ruf, A. May, G. Emig, Applied Catalysis A: General **213**, 203 (2001)
12. Michael Haubs, Klaus Kurzm, Jurgen Lingnau, *Process for the production of trioxane* (2017)
13. M. Sagou, T. Deguchi, S. Nakamura, in *Successful Design of Catalysts Future Requirements and Development, Proceedings ofthe Worldwide Catalysis Seminars, July, 1988, on the Occasion of the 30th Anniversary of the Catalysis Society of Japan* (Elsevier, 1989), p. 139
14. M. Merko, G.W. Busser, M. Muhler, ChemCatChem **14** (2022)
15. A. Musˇicˇ, J. Batista, J. Levec, Applied Catalysis A: General **165**, 115 (1997)
16. Masakazu Sagou, *Process for producing formaldehyde* (1985)
17. M.A. Tadashi Yao, *Production of formaldehyde*
18. V.V. Baghramyan, A.A. Sargsyan, N.V. Gurgenyan, N.B. Knyazyan, V.V. Arutyunyan, E.M. Aleksanyan, N.E. Grigoryan, A.A. Saakyan, Theor Found Chem Eng **52**, 873 (2018)
19. M.F. Casula, D. Loche, S. Marras, G. Paschina, A. Corrias, Langmuir : the ACS journal of surfaces and colloids **23**, 3509 (2007)
20. S. Zhang, L. Hou, M. Hou, H. Liang, Materials Letters **156**, 82 (2015)
21. S. Battiston, C. Rigo, E.C. Da Severo, M.A. Mazutti, R.C. Kuhn, A. Gündel, E.L. Foletto, Mat. Res. **17**, 734 (2014)
22. M. Fabián, P. Bottke, V. Girman, A. Düvel, K.L. Da Silva, M. Wilkening, H. Hahn, P. Heitjans, V. Šepelák, RSC Adv. **5**, 54321 (2015)
23. M. Nadjafi, A.M. Kierzkowska, A. Armutlulu, R. Verel, A. Fedorov, P.M. Abdala, C.R. Müller, J. Phys. Chem. C **125**, 14065 (2021)
24. B.R. Strohmeier, Surface Science Spectra **3**, 128 (1994)
25. L. Su, L. Miao, J. Miao, Z. Zheng, B. Yang, R. Xia, P. Chen, J. Qian, Journal of Asian

Ceramic Societies **4**, 185 (2016)

26. C.-T. Wang, J.-C. Lin, Applied Surface Science **254**, 4500 (2008)
27. F. Pinzari, Reac Kinet Mech Cat **134**, 23 (2021)
28. C.-L. Wang, W.-S. Hwang, H.-L. Chu, H.-H. Ko, C.-S. Hsi, W.-L. Li, K.-M. Chang, M.-C. Wang, Metall and Mat Trans A **45**, 2689 (2014)
29. K. Jothimurugesan, S.K. Gangwal, Ind. Eng. Chem. Res. **37**, 1929 (1998)
30. Y. Ogura, T. Asai, K. Sato, S. Miyahara, T. Toriyama, T. Yamamoto, S. Matsumura, K. Nagaoka, Energy Technol. **8**, 2000264 (2020)
31. M.A. Simonov, P.A. Sandomirskii, Y. Egorov Tismenko, N.V. Belov, Doklady Akademii Nauk SSSR **237**, 581 (1977)
32. B.C. Babu, S. Buddhudu, Physics Procedia **49**, 128 (2013)
33. H.F. Masakazu Sagou, *Process for producing formaldehyde* (1988)
34. M. Takesue, H. Hayashi, R.L. Smith, Progress in Crystal Growth and Characterization of Materials **55**, 98 (2009)
35. R.K. Iler, *The chemistry of silica: Solubility, polymerization, colloid and surface properties, and biochemistry / Ralph K. Iler: Solubility, polymerization, colloid and surface properties, and biochemistry / Ralph K. Iler* (Wiley, New York, Chichester, 1979)
36. Friederike C. Jentoft, *Thermal Treatment of Catalysts: Modern Methods in Heterogeneous Catalysis Research: Modern Methods in Heterogeneous Catalysis Research* (2003)
37. T.S. Norton, F.L. Dryer, Int. J. Chem. Kinet. **22**, 219 (1990)
38. H. Hashemi, J.M. Christensen, S. Gersen, P. Glarborg, Proceedings of the Combustion Institute **35**, 553 (2015)
39. D. Weibel, Z.R. Jovanovic, E. Gálvez, A. Steinfeld, Chemistry of materials : a publication of the American Chemical Society **26**, 6486 (2014)
40. Y. Ren, F. Zhang, W. Hua, Y. Yue, Z. Gao, Catalysis Today **148**, 316 (2009)
41. P. Chen, H.-B. Zhang, G.-D. Lin, Q. Hong, K.R. Tsai, Carbon **35**, 1495 (1997)
42. V. Abdelsayed, M.W. Smith, D. Shekhawat, Applied Catalysis A: General **505**, 365 (2015)
43. A.M. Bahmanpour, F. Héroguel, C.J. Baranowski, J.S. Luterbacher, O. Kröcher, Applied Catalysis A: General **560**, 165 (2018)
44. S. Akhter, Journal of catalysis **85**, 437 (1984)
45. J.M. Vohs, M.A. Barteau, Surface Science **176**, 91 (1986)